Published in final edited form as:
Protein Expr Purif. 2012 September ; 85(1): 25–31. doi:10.1016/j.pep.2012.06.012.

Efficient stable isotope labeling and purification of vitamin D receptor from inclusion bodies

Jinge Zhu[a,1], **Hongyu Rao**[a,1], **Marco Tonelli**[b], **Milo Westler**[b], **Kiran K. Singarapu**[b], **John L. Markley**[a,b], **Hector F. DeLuca**[a,*], and **Fariba M. Assadi-Porter**[a,b,*]

[a]Department of Biochemistry, UW-Madison, 433 Babcock Drive, Madison WI 53706, USA

[b]National Magnetic Resonance Facility at Madison (NMRFAM), University of Wisconsin-Madison, 433 Babcock Drive, Madison WI 53706, USA

Abstract

Vitamin D receptor (VDR) plays a crucial role in many cellular processes including calcium and phosphate homeostasis. Previous purification methods from prokaryotic and eukaryotic expression systems were challenged by low protein solubility accompanied by multi purification steps resulting in poor protein recovery. The full-length VDR and its ligand binding domain (LBD) were mostly (>90%) insoluble even when expressed at low temperatures in the bacterial system. We describe a one-step procedure that results in the purification of rat VDR and LBD proteins in high-yield from *E. coli* inclusion bodies. The heterologously expressed protein constructs retain full function as demonstrated by ligand binding and DNA binding assays. Furthermore, we describe an efficient strategy for labeling these proteins with, ^{13}C, and ^{15}N for structural and functional studies by nuclear magnetic resonance (NMR) spectroscopy. This efficient production system will facilitate future studies on the mechanism of vitamin D action including characterization of the large number of synthetic vitamin D analogs that have been developed.

Keywords

Vitamin D receptor; NMR (Nuclear Magnetic Resonance); Isotope labeling; Inclusion bodies; *E. coli* expression

Introduction

1α,25-Dihydroxyvitamin D_3 [1,25$(OH)_2D_3$], the hormonally active form of vitamin D_3, plays an essential role in calcium and phosphate homeostasis and an important role in specific cell differentiation in the immune system and elsewhere [1–3]. Consequently, vitamin D deficiency has been associated with osteoporosis, cancers, autoimmune disorders,

*To whom correspondence should be addressed: Department of Biochemistry, University of Wisconsin-Madison, 433 Babcock Drive, Madison WI 53706. Phone: (608) 261–1167; Fax: (608) 262–7122; fariba@nmrfam.wisc.edu.
[1]Authors contributed equally to the present work.

Author Contributions H.F.D, W.M.W. initiated the project. F.M.A-P, J.Z., H.R., W.M.W., and H.F.D. designed the research. F.M.A-P designed protein folding and uniform stable isotope labeling protocols, J.Z., and H.R. carried out expression, isotope labeling, and prepared the protein samples. K.K.S. and M.T collected the NMR data. J.Z., H.R., and F. M.A-P analyzed the data and prepared the figures. J.Z, H.R., F.M.A-P, H.F.D. and J.L.M prepared the manuscript. The authors declare no competing financial interests.

cardiovascular diseases, and infections [1–3]. The pleiotropic actions of vitamin D have highlighted $1,25(OH)_2D_3$ and its analogs as potential therapeutic agents in a variety of diseases beyond those relating to calcium, phosphate, and bone [4, 5].

$1,25(OH)_2D_3$ and its analogs exert their function by binding to the vitamin D receptor (VDR), which in turn forms a heterodimer with retinoid X receptor. The ternary complex binds to specific DNA sites on target genes (vitamin D response elements or VDREs) and recruits an array of various co-activators and co-repressors that regulate gene expression [6]. Defects in the VDR gene causes hereditary vitamin D resistant rickets type II (HVDRR) [7]. Genetic ablation of VDR in mice leads to phenotypic traits characteristic of HVDRR as a result of loss of hormonal control [8–11].

VDR is highly conserved among vertebrates ranging from fish to human and displays broad tissue distribution with the highest expression in the intestine. Nevertheless, coinciding with the subnanomolar affinity for its natural ligand, VDR is present in low abundance, making direct purification difficult [12–14]. The VDR genes from multiple species have been cloned [15–22], and the heterologous expression and purification of recombinant VDR has facilitated its biochemical characterization and extended our understanding of the mechanism of vitamin D action [23–30]. Crystallographic studies of VDR have provided insight into its structure-activity relationships [31–34]. However, it remains unclear why VDR in complex with $1,25(OH)_2D_3$ and its analogs having distinct structures and unique biological effects, exhibit essentially the same protein structure in X-ray crystal studies [32, 35–40]. Nuclear magnetic resonance (NMR) studies on VDR have been limited [29], largely owing to the unavailability of active and stable proteins in sufficient quantity. Previous purification of soluble forms of VDR or its ligand binding domain (LBD) from prokaryotic and eukaryotic systems usually involved time consuming multistep purification protocols to achieve adequate purity. Subsequently, after final removal of the purification tag the overall yield was rather low [23–30].

In this study, we describe an efficient overexpression and one-step purification protocol with high yields (25–70 mg/L culture) for full-length VDR and LBD proteins that allows economically feasible isotope labeling strategies required for structure-function characterization of these large molecular weight proteins by NMR spectroscopy.

Materials and methods

Reagents

All isotopic labeled ISOGRO® Complex Growth Media were purchased from ISOTEC™ (Sigma-Aldrich). Ammonium chloride (^{15}N, 99%), D-glucose (1,2,3,4,5,6,6-D7, 98%), and D-glucose (U-^{13}C6, 99%; 1,2,3,4,5,6,6-D7, 97–98%) were purchased from Cambridge Isotope Laboratories. Deuterium oxide (99% D), isopropyl-β-D-thiogalactopyranoside (IPTG), and dithiothreitol (DTT) were from Sigma-Aldrich. $1,25(OH)_2D_3$ was purchased from SAFC-Pharma (Madison, WI). 26,27-[^3H]-$1,25(OH)_2D_3$ was provided by Perkin-Elmer (Boston, MA). All other chemicals were from Fisher or Sigma.

Plasmid constructs and E. coli expression strains

Plasmid p29LBD codes for the production of rat VDR LBD residues 116–423 (Fig. 1) with a C-terminal six-histidine tag flanked by a linker sequence containing a thrombin cleavage site [29]. Plasmid p29LBDm is derived from p29LBD as previously described [32]. This new construct encodes LBD in which the flexible 47 amino acid (165–211) loop has been truncated. Plasmid p29LBDm-NT is derived from p29LBDm without the C-terminal His-tag. Constructs p29VDR, p29VDRm, and p29VDRm-NT are the full-length counterparts of p29LBD, p29LBDm, and p29LBDm-NT; we refer to these constructs as VDR, VDRm,

VDRm-NT and LBD, LBDm, LBDm-NT, respectively. *E. coli* strains Rosetta 2(DE3) (Novagen, Madison, WI, USA) and BL21-CodonPlus(DE3)-RIPL (Stratagene, Agilent Technologies, Inc., Santa Clara, CA, USA) are designated as Rosetta and BL21/RIPL, respectively.

Expression media

Luria broth (LB) medium was used as a control for recombinant protein expression, and M9 minimal medium was the basis for stable isotope labeling. For deuterium labeling, H_2O based M9 was replaced with 99% D_2O based M9 supplemented with 1 mL/L 100× BME vitamin solution (Sigma-Aldrich, St. Louis, MO, US), 200 mM $MgSO_4$, 100 μM $CaCl_2$, and 0.2% D-glucose (1,2,3,4,5,6,6-D7, 98%) as the sole carbon source. For additional isotope labeling, $^{15}NH_4Cl$ and/or D-glucose (U-^{13}C6, 99%; 1,2,3,4,5,6,6-D7, 97–98%) were used. To improve the expression of isotopically-labeled VDR and LBD, 0.5% ISOGRO (5 g/L) was added as a supplement to the M9 medium, and the pH was adjusted to 7.2. Kanamycin and chloramphenicol were added to final concentrations of 50 μg/L and 34 μg/L, respectively, for antibiotic selection.

Expression of LBD and VDR

LBD and VDR were expressed as previously described [24–27] with some modifications. Chemically competent cells of BL21/RIPL and Rosetta were freshly transformed with the desired DNA construct following the general DNA transformation method. A starter culture in LB (20 mL) was inoculated with single colonies and grew at 30 °C overnight. The starting culture was added to 1 L of expression media (LB, M9 or 0.5% ISOGRO) with (50 μg/mL) kanamycin and (34 μg/mL) chloramphenicol and grown at 37 °C until A600 nm of 0.5–0.8 was reached. Cells were induced by addition of IPTG to a final concentration of 250 μM. Temperature after induction was varied to 18 °C, 23 °C, 30 °C or 37 °C, and the cultures were allowed to grow for up to 24 h. The cells were harvested by centrifugation at 2,500 × g at 4 °C for 20 min and rinsed with 0.9% (w/v) NaCl. The protein expression was analyzed by sodium dodecyl sulfate polyacrylamide gel electrophoresis (SDS-PAGE).

Purification of LBD and VDR from inclusion bodies

The refolding protocol from inclusion bodies was specifically modified for chemical properties of VDR and is based on the previous method of refolding used in nuclease-brazzein fusion protein [41]. The refolding protocol was particularly modified for the first time to account for the p*I and redox state of cysteines* of VDR or LBD. These modifications included adjustment for buffer, pH, and addition of reducing agent to keep free cysteines in VDR in the reduced state. Briefly, the cell pellet prepared above was suspended in lysis buffer (50 mM Tris-HCl, pH 8.0, 10 mM DTT, 0.3 mM phenylmethylsulfonyl fluoride, and 0.5 mg/mL lysozyme). Cells were sonicated with a sonic dismembrator (Fisher, Hanover Park, IL, USA) followed by centrifuging at 14,000g at 4 °C for 15 min. Cell pellets including inclusion bodies were washed once with 9 volumes of wash buffer (50 mM Tris-HCl, pH 8.0, and 100 mM NaCl), and once with the same wash buffer containing 0.5% (v/v) Triton X-100. After each addition, the slurry was stirred gently for 5 min and then centrifuged at 21,000 × g at 4 °C for 20 min. The final pellet was resuspended gently in 6 M guanidinium chloride dissolved in 40 mM Tris-acetate (pH 7.6) containing 100 mM DTT, and stirred for 2~3 h at room temperature. A clear solution was achieved by centrifugation at 21,000 × g at 4 °C for 20 min. The supernatant was dialyzed against 100 volumes of dialysis buffer containing 25 mM NaH_2PO_4/Na_2HPO_4 (pH 7.4), 50 mM KCl, and 2 mM DTT at 4 °C overnight followed by two more changes of the same buffer over 24 h to remove the denaturant and the reducing agent. The protein solution was concentrated to a final protein concentration of 0.5–1 mg/mL in an Amicon centrifugal filter (Millipore Ireland Ltd, Tullagreen, Carrigtwohill CO. CORK IRL).

The purity of the protein was analyzed by 12% SDS-PAGE. The yield of the protein was measured by the Bradford method (Bio-Rad, Hercules, CA). The protein was further characterized by electrospray ionization mass spectrometry (ESI-MS) at the University of Wisconsin Biotechnology Center.

Ligand binding assay

Ligand binding activity was determined using a competition assay as previously described [42]. Briefly, VDR or LBD (final 1 nM) was incubated with 0.16 μCi/mL 26,27-[^{3}H]-1,25(OH)$_2$D$_3$ (157.9 Ci/mmol) and increasing concentrations of 1,25(OH)$_2$D$_3$ on ice overnight in a buffer containing 50 mM Tris (pH 7.4), 1.5 mM EDTA, 150 mM KCl, 5 mM DTT and 0.2 % CHAPS. Hydroxyapatite gel (Bio-Rad, Hercules, CA) as 50% slurry was added and mixed at 10 min intervals for 30 min to bind the protein. The resin was washed three times with a buffer containing 50 mM Tris (pH 7.4), 1.5 mM EDTA and 0.5% Triton X-100, and subjected to tritium count after mixed in Bio-Safe II scintillation cocktail. The binding curve was fitted in a single site competitive binding model using Prism 5.0. All assays were performed in duplicate.

DNA binding

A gel filtration assay was used to assess the DNA binding activity of VDR [34]. VDRm-NT (3-fold molar excess) was incubated with an oligonucleotide duplex with a sense sequence of 5′-CACGGTTCACGAGGTTCACAC-3′ (VDRE half-site underlined) in a buffer containing 20 mM NaH_2PO_4/Na_2HPO_4 (pH 7.4), 50 mM KCl and 2 mM DTT overnight on ice. Each oligonucleotide strand (Integrated DNA Technologies) was HPLC purified and annealed by heating at 95 °C for 7 min and gradually cooling down to room temperature. The mixture was applied to a Sephadex G-200 column (1.6 × 24 cm) (Pharmacia, GE Healthcare, Pittsburgh, USA), eluted with a buffer containing 10 mM Tris (pH 7.5) and 62.5 mM NaCl, collected and monitored by UV absorption at 280 nm. The fractions containing DNA and/or protein were concentrated and analyzed on 0.8% TAE agarose gel containing 0.02% ethidium bromide. For western blot, the fractions were run by 12% SDS-PAGE and transferred onto a nitrocellulose membrane (Bio-Rad, Hercules, CA). The blot was blocked with 6% bovine serum albumin in Tris-HCl buffered saline containing 0.05% TWEEN® 20 at room temperature for 1 h and then incubated with 0.2 μg/mL mouse monoclonal VDR (D-6) antibody (sc-13133, Santa Cruz Biotechnology, Santa Cruz, CA) in the same buffer at 4 °C overnight. After thorough washing, the secondary antibody of goat anti-mouse IgG light chain conjugated with horseradish peroxidase (Jackson ImmunoResearch Laboratories, West Grove, PA) was added and allowed to incubate at room temperature for 1 h. The signals were detected using Amersham ECL western blotting analysis system (GE Healthcare, Buchinghamshire, UK) followed by development on X-ray films (Kodak). For gel mobility shift, the DNA fragment was incubated in the absence and presence of increasing concentrations of VDRm-NT (up to 8-fold molar excess) at 4 °C for 2 h and analyzed on 0.8% TAE agarose gel followed by brief staining in 0.1% ethidium bromide bath.

NMR spectroscopy sample preparation and NMR spectroscopy

All NMR spectra were recorded using a Varian 900 MHz (^{1}H) spectrometer equipped with a cryogenic probe with the temperature regulated at 25 °C on ~0.5 mM samples of labeled VDR in 20 mM NaH_2PO_4-Na_2HPO_4 (pH 7.4), 50 mM KCl, 5 mM DTT, 5X protease inhibitor (Roche, address), 0.05% NaN_3, and 7% D_2O. A 4-fold molar excess of the 13-residue peptide from DRIP205, which contains the LxxLL motif mimicking the co-activator was added to the final NMR sample [43] prior to data collection. To better estimate level of perdeuteration, TROSY (transverse relaxation-optimized spectroscopy) based ^{15}N resolved

3D-^{1}H,^{1}H NOESY spectra were collected. All spectra were processed with NMRPipe (http://spin.niddk.nih.gov/NMRPipe/).

Results

Plasmid constructs to express VDR and LBD

The coding sequences for VDR and LBD variants (Fig. 1) were constructed in the T7 promoter-driven pET-29b(+) vector (Novagen, Madison, WI, USA) for IPTG-inducible expression. The flexible insertion loop coding for amino acid residues 165–211 (Fig. 1) was deleted in the constructs p29VDRm and p29LBDm to remove the flexible loop region without compromising the ligand binding activity (*vide infra*), dimerization or transactivation function [31, 44].

Expression and solubility of natural abundance and deuterated VDR and LBD

The production levels of VDR and LBD in LB, M9 and 0.5% ISOGRO media prepared in H_2O and D_2O are compared in Fig. 2. Both proteins showed high levels of production in all media tested in this study. However, the majority of protein over-expressed under different medium and temperature conditions (18–37 °C) was found in the inclusion bodies. 37 °C was chosen as the culture temperature to achieve optimal protein production level and cell density. Two *E. coli* strains, BL21/RIPL and Rosetta, were tested for production of VDR and LBD. Rosetta exhibited moderately superior yields of full-length VDR protein to BL21/RIPL (data not shown). However, both strains produced the shorter length LBD protein equally well (data not shown).

Purification and yield of VDR and LBD in rich and deuterated minimal media

The purity and yield of purified VDRm and LBDm are shown in Fig. 3 and Table 1. The yield for LBD protein was 70 mg/L of LB (data not shown), whereas the yields for each of VDRm or LBDm were 32–35 mg/L (~25% recovery from inclusion bodies), respectively. The yields of VDRm or LBDm produced in 0.5% ISOGRO in D_2O were both 25 mg/L. Mass spectrometry of unlabeled proteins showed that the molecular weights of the purified LBD and VDR proteins matched those expected (29,706 and 42,952, data not shown). Mass spectrometry of various double or triple labeled samples revealed isotope incorporation of 96.4% ^{2}H, 96.6% ^{13}C and 96.6% ^{15}N.

Ligand binding and DNA binding activity

A hydroxyapatite binding assay was used to measure the ligand binding activity of VDR and LBD [42]. As shown in Fig. 4 and Table 2, all VDR and LBD variants exhibited similar binding affinity toward the natural ligand 1,25$(OH)_2D_3$ with dissociation constants of 0.19–0.25 nM, consistent with previously determined values [6]. Incubation of VDRm-NT with a DNA duplex containing VDRE sequence resulted in gel mobility shift shown in Fig. 5, indicating effective DNA binding. These results demonstrated that the refolded VDR and LBD retained their full function as those purified by other methods previously [23–30].

Folding and deuterium isotopic labeling incorporation by NMR

The efficiency of deuterium isotopic labeling for [U-^{2}H,^{13}C,^{15}N]-VDR was further verified by three-dimensional (3D) NOESY ^{1}H,^{15}N HSQC-TROSY. A two-dimensional (2D) ^{1}H-^{1}H projection is shown in Fig. 6. The suppression of ^{1}H signals in the aliphatic region (~0–6.0 ppm) indicates that the labeled [U-^{2}H,^{13}C,^{15}N]-VDR sample is highly deuterated. On the other hand, the amide proton region (6.5–8.5 ppm) showed many well-dispersed signals indicating a well-folded protein (Fig. 6). Similar results were observed for [U-^{2}H,^{13}C,^{15}N]-LBD (data not shown) [43].

Discussion

Crystallography and solution NMR are the two methods available for determining three-dimensional (3D) structure at atomic resolution to gain knowledge about protein function and its mechanism of action. NMR solution studies can provide additional information, such as solution state dynamics and conformational equilibria, which cannot be obtained through X-ray crystallography [45–47]. In the case of LBD, significant differences were found between ligand-bound structures in the crystal state and in solution [43]. Because of their large sizes, VDR (>40 kDa) and LBD (~30 kDa), >90% uniform deuteration in addition to ^{15}N and ^{13}C labeling is required for structural analysis. In addition, a large quantity of labeled protein (5~10 mg for VDR, 3~5 mg for LBD) is needed for detailed NMR investigations [48]. Protein purification at high homogeneity is also required.

The first VDR gene was cloned more than two decades ago [15–17], but only a few structures of LBD and the DNA binding domain have been determined [31–34], largely due to either insufficient protein yield or stability. Initial purification of VDR was from eukaryotic systems, such as yeast and insect cells, which required time consuming, multi-step chromatography methods to achieve adequate purity. The removal of the purification tag afterward further reduced recovery yields (0.5–3.5 mg/L) [23, 24, 27, 28, 30]. Subsequently, the purification of VDR or LBD from *E. coli* was reported, but yields were low because only the small soluble fraction was utilized [25, 26, 29, 31, 32]. These production systems were not economically conducive for NMR studies that require deuterium isotope labeling and fairly concentrated samples.

In our study, we found that most of the VDR and LBD proteins produced in *E. coli* were in inclusion bodies (Fig. 2B). We developed a highly efficient protein refolding protocol that allowed recovery of VDR from the inclusion bodies (Table 1), with yields up to 30–70 times higher than previous methods. In addition, the refolded VDR and LBD retained full function as verified by NMR ligand binding [43] and DNA binding assays (Table 2, Figs. 4 and 5).

In addition, we discovered an efficient method for producing [U-^{2}H,^{13}C,^{15}N]-VDR and [U-^{2}H,^{13}C,^{15}N]-LBD. The labeled samples were highly deuterated and well folded as clearly indicated by the NOESY ^{1}H,^{15}N HSQC-TROSY NMR data. Furthermore, these samples were stable in NMR tubes over several months [43]. The new high efficiency expression and purification method will open avenues to other important characterization methods and biological studies on VDR, which together with NMR techniques will further facilitate its biochemical and biophysical characterization to improve our understanding of the mechanism of vitamin D action. For proteins that are large (>25 kDa) and locate mainly in inclusion bodies, the VDR refolding protocol described here may offer an efficient purification approach to increasing yields.

Acknowledgments

This paper is dedicated to the memory of Norma Marchesini. This research was supported by R01 DC009018 to FAP, funding from the Wisconsin Alumni Research Foundation to HFD, and NIH grants (to JLM) from the National Center for Research Resources (5P41RR002301-27 and RR02301-26S1) and the National Institute for General Medical Sciences (8 P41 GM103399-27) that support the National Magnetic Resonance Facility at Madison where NMR data were collected.

Abbreviations

$1,25(OH)_2D_3$	1α,25-dihydroxyvitamin D_3
VDR	vitamin D receptor

VDRE	vitamin D response element
HVDRR	hereditary vitamin D resistant rickets
NMR	nuclear magnetic resonance
LBD	ligand binding domain
IPTG	isopropyl-β-D-thiogalactopyranoside
DTT	dithiothreitol
LB	Luria broth
SDS-PAGE	sodium dodecyl sulfate polyacrylamide gel electrophoresis

References

1. DeLuca HF. Evolution of our understanding of vitamin D. Nutr Rev. 2008; 66:S73–S87. [PubMed: 18844850]
2. Holick MF. The vitamin D deficiency pandemic and consequences for nonskeletal health: mechanisms of action. Mol Aspects Med. 2008; 29:361–368. [PubMed: 18801384]
3. Bikle D. Nonclassic actions of vitamin D. J Clin Endocrinol Metab. 2009; 94:26–34. [PubMed: 18854395]
4. Jones, G. Vitamin D and analogues. In: Bilezikian, JP.; Raisz, LG.; Martin, TJ., editors. Principles of Bone Biology. 3. Vol. 2. Elsevier Academic Press; 2008. p. 1777-1799.
5. Brown A, Slatopolsky E. Vitamin D analogs: therapeutic applications and mechanisms for selectivity. Mol Aspects Med. 2008; 29:433–452. [PubMed: 18554710]
6. Pike, JW.; Shevde, NK. The vitamin D receptor. In: Feldman, D.; Pike, JW.; Glorieux, FH., editors. Vitamin D. 2. Vol. 1. Elsevier Academic Press; 2005. p. 167-191.
7. Malloy, PJ.; Pike, JW.; Feldman, D. Hereditary 1,25-dihydroxyvitamin D-resistant rickets. In: Feldman, D.; Pike, JW.; Glorieux, FH., editors. Vitamin D. 2. Vol. 1. Elsevier Academic Press; 2005. p. 1207-1237.
8. Li YC, Pirro AE, Amling M, Delling G, Baron R, Bronson R, Demay MB. Targeted ablation of the vitamin D receptor: an animal model of vitamin D-dependent rickets type II with 3alopecia. Proc Natl Acad Sci USA. 1997; 94:9831–9835. [PubMed: 9275211]
9. Yoshizawa T, Handa Y, Uematsu Y, Takeda S, Sekine K, Yoshihara Y, Kawakami T, Arioka K, Sato H, Uchiyama Y, Masushige S, Fukamizu A, Matsumoto T, Kato S. Mice lacking the vitamin D receptor exhibit impaired bone formation, uterine hypoplasia and growth retardation after weaning. Nat Genet. 1997; 16:391–396. [PubMed: 9241280]
10. Van Cromphaut SJ, Dewerchin M, Hoenderop JGJ, Stockmans I, Van Herck E, Kato S, Bindels RJM, Collen D, Carmeliet P, Bouillon R, Carmeliet G. Duodenal calcium absorption in vitamin D receptor–knockout mice: functional and molecular aspects. Proc Natl Acad Sci USA. 2001; 98:13324–13329. [PubMed: 11687634]
11. Erben RG, Soegiarto DW, Weber K, Zeitz U, Lieberherr M, Gniadecki R, Möller G, Adamski J, Balling R. Deletion of deoxyribonucleic acid binding domain of the vitamin D receptor abrogates genomic and nongenomic functions of vitamin D. Mol Endocrinol. 2002; 16:1524–1537. [PubMed: 12089348]
12. Pike JW, Haussler MR. Purification of chicken intestinal receptor for 1,25-dihydroxyvitamin D. Proc Natl Acad Sci USA. 1979; 76:5485–5489. [PubMed: 230478]
13. Simpson RU, DeLuca HF. Purification of chicken intestinal receptor for 1α,25-dihydroxyvitamin D_3 to apparent homogeneity. Proc Natl Acad Sci USA. 1982; 79:16–20. [PubMed: 6275386]
14. Dame MC, Pierce EA, Prahl JM, Hayes CE, DeLuca HF. Monoclonal antibodies to the porcine intestinal receptor for 1,25-dihydroxyvitamin D_3: interaction with distinct receptor domains. Biochemistry. 1986; 25:4523–4534. [PubMed: 2429689]

15. McDonnell DP, Mangelsdorf DJ, Pike JW, Haussler MR, O'Malley BW. Molecular cloning of complementary DNA encoding the avian receptor for vitamin D. Science. 1987; 235:1214–1217. [PubMed: 3029866]
16. Baker AR, McDonnell DP, Hughes M, Crisp TM, Mangelsdorf DJ, Haussler MR, Pike JW, Shine J, O'Malley BW. Cloning and expression of full-length cDNA encoding human vitamin D receptor. Proc Natl Acad Sci USA. 1988; 85:3294–3298. [PubMed: 2835767]
17. Burmester JK, Maeda N, DeLuca HF. Isolation and expression of rat 1,25-dihydroxyvitamin D_3 receptor cDNA. Proc Natl Acad Sci USA. 1988; 85:1005–1009. [PubMed: 2829212]
18. Elaroussi MA, Prahl JM, DeLuca HF. The avian vitamin D receptors: primary structures and their origins. Proc Natl Acad Sci USA. 1994; 91:11596–11600. [PubMed: 7972109]
19. Kamei Y, Kawada T, Fukuwatari T, Ono T, Kato S, Sugimoto E. Cloning and sequencing of the gene encoding the mouse vitamin D receptor. Gene. 1995; 152:281–282. [PubMed: 7835717]
20. Li YC, Bergwitz C, Juppner H, Demay MB. Cloning and characterization of the vitamin D receptor from *Xenopus laevis*. Endocrinology. 1997; 138:2347–2353. [PubMed: 9165021]
21. Suzuki T, Suzuki N, Srivastava AS, Kurokawa T. Identification of cDNAs encoding two subtypes of vitamin D receptor in flounder,*Paralichthys olivaceus*. Biochem Biophys Res Commun. 2000; 270:40–45. [PubMed: 10733902]
22. Whitfield GK, Dang HTL, Schluter SF, Bernstein RM, Bunag T, Manzon LA, Hsieh G, Dominguez CE, Youson JH, Haussler MR, Marchalonis JJ. Cloning of a functional vitamin D receptor from the lamprey (*Petromyzon marinus*), an ancient vertebrate lacking a calcified skeleton and teeth. Endocrinology. 2003; 144:2704–2716. [PubMed: 12746335]
23. Sone T, McDonnell DP, O'Malley BW, Pike JW. Expression of human vitamin D receptor in *Saccharomyces cerevisiae*. Purification, properties, and generation of polyclonal antibodies. J Biol Chem. 1990; 265:21997–22003. [PubMed: 2174892]
24. Li Z, Prahl JM, Hellwig W, DeLuca HF. Immunoaffinity purification of active rat recombinant 1,25-dihydroxyvitamin D_3 receptor. Arch Biochem Biophys. 1994; 310:347–351. [PubMed: 8179318]
25. Hsieh J-C, Nakajima S, Galligan MA, Jurutka PW, Haussler CA, Whitfield GK, Haussler MR. Receptor mediated genomic action of the $1,25(OH)_2D_3$ hormone: expression of the human vitamin D receptor in *E. coli*. J Steroid Biochem Mol Biol. 1995; 53:583–594. [PubMed: 7626514]
26. Strugnell SA, Hill JJ, McCaslin DR, Wiefling BA, Royer CA, DeLuca HF. Bacterial expression and characterization of the ligand-binding domain of the vitamin D receptor. Arch Biochem Biophys. 1999; 364:42–52. [PubMed: 10087163]
27. Juntunen K, Rochel N, Moras D, Vihko P. Large-scale expression and purification of the human vitamin D receptor and its ligand-binding domain for structural studies. Biochem J. 1999; 344:297–303. [PubMed: 10567209]
28. Jurutka PW, MacDonald PN, Nakajima S, Hsieh J-C, Thompson PD, Whitfield GK, Galligan MA, Haussler CA, Haussler MR. Isolation of baculovirus-expressed human vitamin D receptor: DNA responsive element interactions and phosphorylation of the purified receptor. J Cell Biochem. 2002; 85:435–457. [PubMed: 11948698]
29. Sicinska W, Westler WM, DeLuca HF. NMR assignments of tryptophan residue in apo and holo LBD-rVDR. Proteins. 2005; 61:461–467. [PubMed: 16130132]
30. Abdulrahman W, Uhring M, Kolb-Cheynel I, Garnier J-M, Moras D, Rochel N, Busso D, Poterszman A. A set of baculovirus transfer vectors for screening of affinity tags and parallel expression strategies. Anal Biochem. 2009; 385:383–385. [PubMed: 19061853]
31. Rochel N, Wurtz JM, Mitschler A, Klaholz B, Moras D. The crystal structure of the nuclear receptor for vitamin D bound to its natural ligand. Mol Cell. 2000; 5:173–179. [PubMed: 10678179]
32. Vanhooke JL, Benning MM, Bauer CB, Pike JW, DeLuca HF. Molecular structure of the rat vitamin D receptor ligand binding domain complexed with 2-carbon-substituted vitamin D_3 hormone analogues and a LXXLL-containing coactivator peptide. Biochemistry. 2004; 43:4101–4110. [PubMed: 15065852]
33. Ciesielski F, Rochel N, Mitschler A, Kouzmenko A, Moras D. Structural investigation of the ligand binding domain of the zebrafish VDR in complexes with $1\alpha,25(OH)_2D_3$ and Gemini:

purification, crystallization and preliminary X-ray diffraction analysis. J Steroid Biochem Mol Biol. 2004; 89–90:55–59.

34. Shaffer PL, Gewirth DT. Structural basis of VDR-DNA interactions on direct repeat response elements. EMBO J. 2002; 21:2242–2252. [PubMed: 11980721]
35. Tocchini-Valentini G, Rochel N, Wurtz JM, Mitschler A, Moras D. Crystal structures of the vitamin D receptor complexed to superagonist 20-epi ligands. Proc Natl Acad Sci USA. 2001; 98:5491–5496. [PubMed: 11344298]
36. Tocchini-Valentini G, Rochel N, Wurtz J-M, Moras D. Crystal structures of the vitamin D nuclear receptor liganded with the vitamin D side chain analogues calcipotriol and seocalcitol, receptor agonists of clinical importance. Insights into a structural basis for the switching of calcipotriol to a receptor antagonist by further side chain modification. J Med Chem. 2004; 47:1956–1961. [PubMed: 15055995]
37. Eelen G, Verlinden L, Rochel N, Claessens F, De Clercq P, Vandewalle M, Tocchini-Valentini G, Moras D, Bouillon R, Verstuyf A. Superagonistic action of 14-epi-analogs of 1,25-dihydroxyvitamin D explained by vitamin D receptor-coactivator interaction. Mol Pharmacol. 2005; 67:1566–1573. [PubMed: 15728261]
38. Vanhooke JL, Tadi BP, Benning MM, Plum LA, DeLuca HF. New analogs of 2-methylene-19-nor-(20*S*)-1,25-dihydroxyvitamin D_3 with conformationally restricted side chains: evaluation of biological activity and structural determination of VDR-bound conformations. Arch Biochem Biophys. 2007; 460:161–165. [PubMed: 17227670]
39. Hourai S, Rodrigues LC, Antony P, Reina-San-Martin B, Ciesielski F, Magnier BC, Schoonjans K, Mouriño A, Rochel N, Moras D. Structure-based design of a superagonist ligand for the vitamin D nuclear receptor. Chem Biol. 2008; 15:383–392. [PubMed: 18420145]
40. Nakabayashi M, Yamada S, Yoshimoto N, Tanaka T, Igarashi M, Ikura T, Ito N, Makishima M, Tokiwa H, DeLuca HF, Shimizu M. Crystal structures of rat vitamin D receptor bound to adamantyl vitamin D analogs: structural basis for vitamin D receptor antagonism and partial agonism. J Med Chem. 2008; 51:5320–5329. [PubMed: 18710208]
41. Assadi-Porter FM, Aceti DJ, Cheng H, Markley JL. Efficient production of recombinant brazzein, a small, heat-stable, sweet tasting protein of plant origin. Arch Biochem Biophys. 2000; 376:252–258. [PubMed: 10775410]
42. Glebocka A, Sicinski RR, Plum LA, Clagett-Dame M, DeLuca HF. New 2-alkylidene 1α,25-dihydroxy-19-norvitamin D_3 analogues of high intestinal activity: synthesis and biological evaluation of 2-(3′-alkoxypropylidene) and 2-(3′-hydroxypropylidene) derivatives. J Med Chem. 2006; 49:2909–2920. [PubMed: 16686534]
43. Singarapu KK, Zhu J, Tonelli M, Rao H, Assadi-Porter FM, Westler WM, DeLuca HF, Markley JL. Ligand-specific structural changes in the vitamin D receptor in solution. Biochemistry. 2011:11025–33. [PubMed: 22112050]
44. Rochel N, Tocchini-Valentini G, Egea PF, Juntunen K, Garnier J-M, Vihko P, Moras D. Functional and structural characterization of the insertion region in the ligand binding domain of the vitamin D nuclear receptor. Eur J Biochem. 2001; 268:971–979. [PubMed: 11179963]
45. Clore GM, Gronenborn AM. Three- and four-dimensional heteronuclear NMR spectroscopy. Science. 1991; 25:1390–1399. [PubMed: 2047852]
46. Mittermaier A, Kay LE. Review – new tools provide new insights in NMR studies of protein dynamics. Science. 2006; 312:224–228. [PubMed: 16614210]
47. Palmer AG. A topical issue: NMR investigations of molecular dynamics. J Biomol NMR. 2009; 45:1–4. [PubMed: 19669621]
48. Sattler M, Fesik SW. Use of deuterium labeling in NMR: overcoming a sizeable problem. Structure. 1996; 4:1245–1249. [PubMed: 8939758]

1. Expression of Vitamin D receptor and its subdomains in *E. coli*.
2. Efficient purification was achieved from inclusion bodies.
3. Full function retained by ligand binding and DNA binding assays.
4. An efficient ^{2}H, ^{13}C, and ^{15}N labeling is described.

Figure 1.

Domain organization of full length VDR. The scheme shows that VDR consists of several domains, including a DNA binding domain (DBD; C domain) and a ligand binding domain (LBD; E domain), linked by a hinge region (D domain) and preceded by a short A/B domain at the N-terminus. The area indicated by the cross in LBD denotes the flexible insertion region that was removed for the NMR studies. The numbers designate amino acid residues in rat VDR.

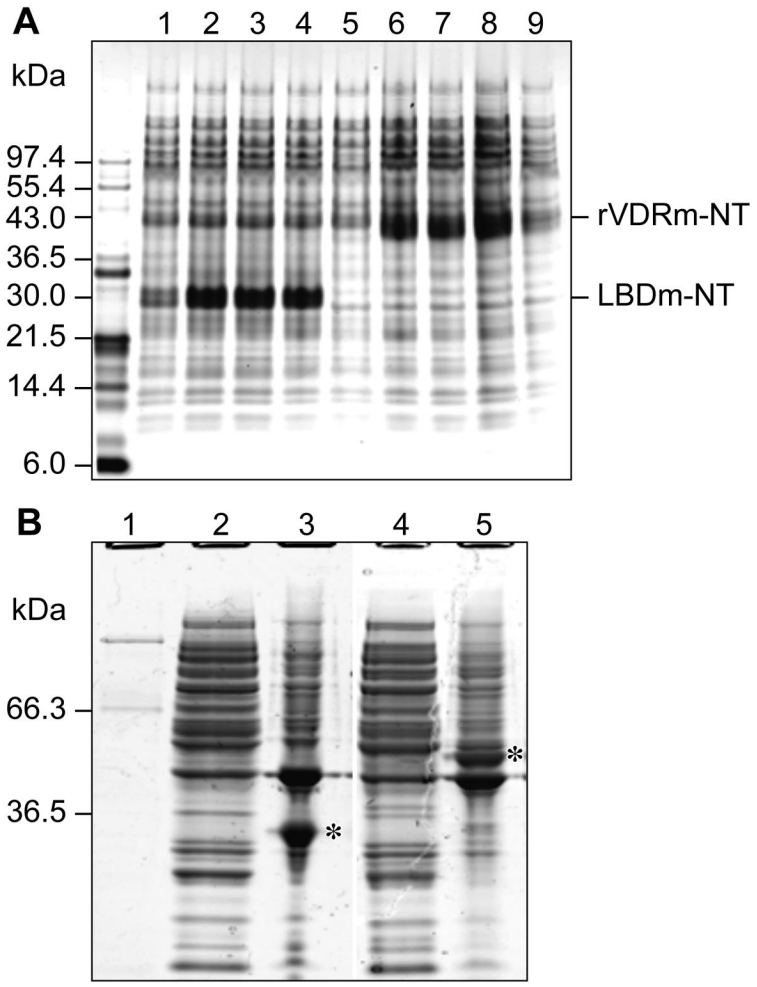

Figure 2.

(A) Expression of LBDm-NT and VDRm-NT in different media analyzed by 16% SDS-PAGE using whole cell lysates. Lanes 1 & 9: +IPTG, 0.5% ISOGRO [U-^{2}H,^{15}N]; lanes 2 & 8: +IPTG, 0.5% ISOGRO [U-^{13}C,^{15}N]; lanes 3 & 7: +IPTG, M9 [U-^{15}N]; lanes 4 & 6: +IPTG, LB; lane 5: -IPTG, LB. (B) Solubility of VDRm-NT and LBDm-NT analyzed by SDS-PAGE. VDRm-NT and LBDm-NT were expressed in LB at 30°C for 6 h using Rosetta and BL21/RIPL as host strains, respectively. Lane 1: soluble part of the whole cell lysate expressing VDRm-NT, lane 2: insoluble part (inclusion body) of the whole cell lysate expressing VDRm-NT, lane 3: soluble part of the whole cell lysate expressing LBDm-NT, lane 4: insoluble part (inclusion body) of the whole cell lysate expressing LBDm-NT.

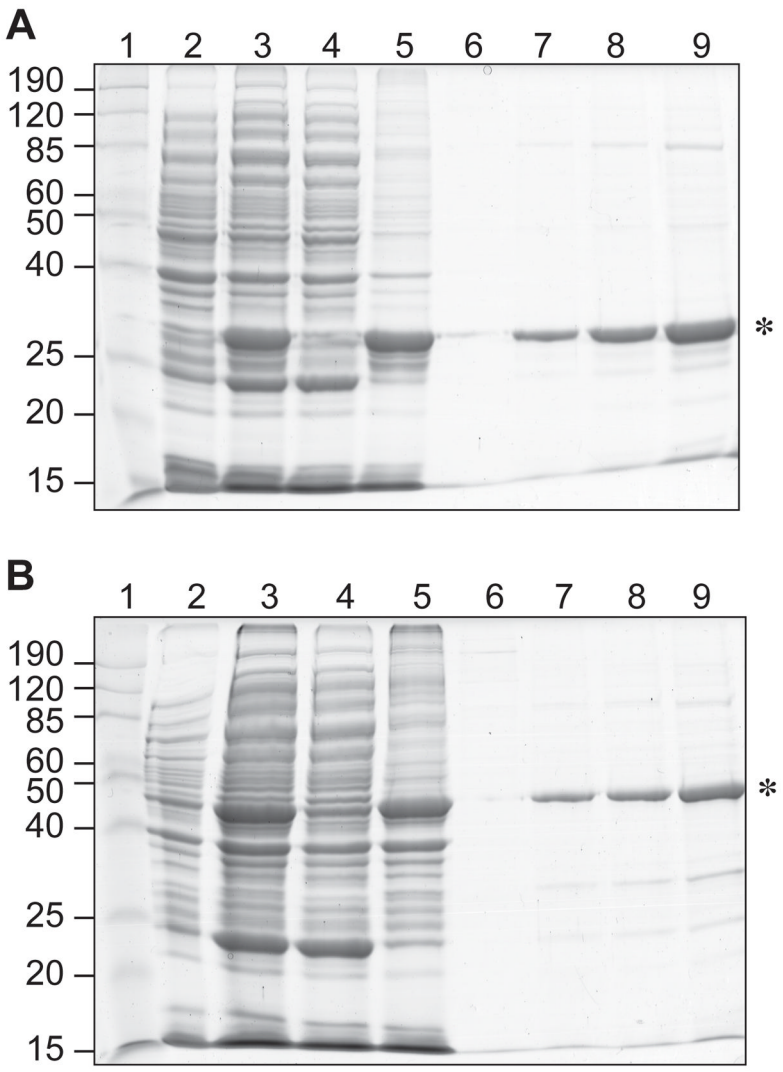

Figure 3.

SDS-PAGE analysis of the production of (A) LBDm-NT and (B) VDRm-NT in rich LB medium. Lane 1: molecular weight markers, lane 2: −IPTG, lane 3: total cell lysate from IPTG induced cells, lanes 4:, soluble supernatant fraction, lane 5: inclusion bodies, lane 6: pooled supernatant, after washing the pellet twice, lane 7–9: purified final recover protein (indicated by *) at 1.5, 3 and 6 μg/lane loadings after dialysis of the redissolved pellet.

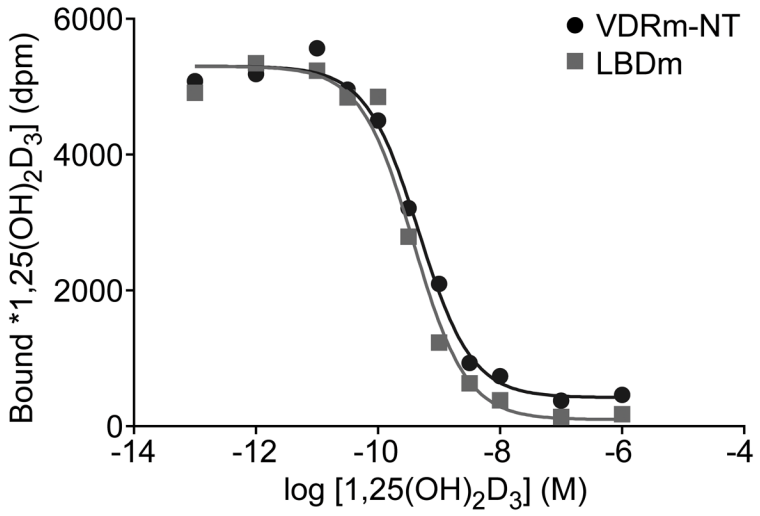

Figure 4.
Competitive ligand binding assay to determine the binding affinity of VDR and LBD variants toward $1,25(OH)_2D_3$. Two representative experiments using VDRm-NT and LBDm are shown (see *Materials and Methods*).

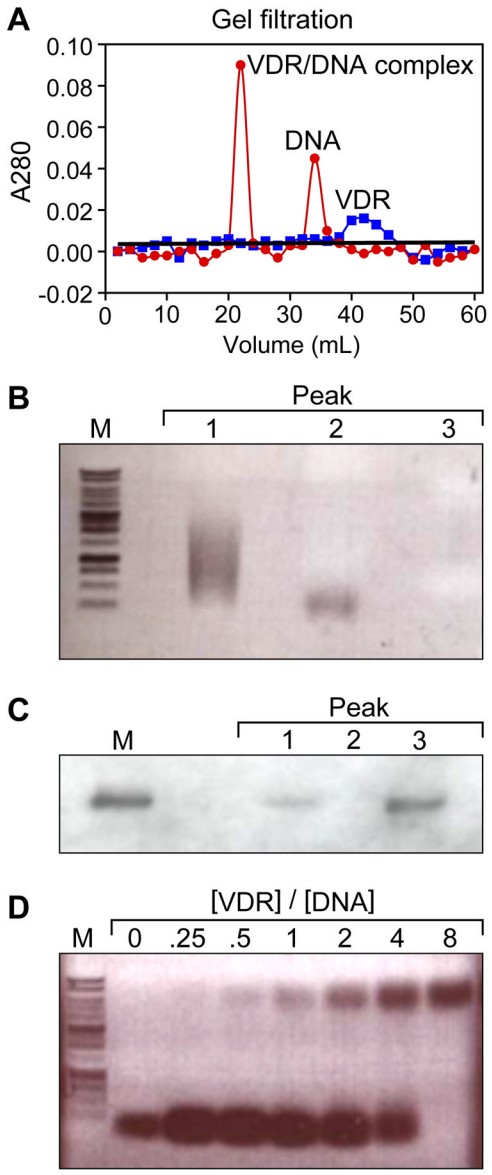

Figure 5.

(A) Elution profile of VDRm-NT and DNA mixture from Sephadex G-200 monitored by UV absorption at 280 nm (red trace). Because of the much lower extinction coefficient of protein compared to that of DNA, the retention time of unbound VDRm-NT was determined using concentrated VDRm-NT in a parallel experiment (blue trace). (B) Agarose gel electrophoresis and (C) western blot confirmed that the fractions in the order of elution contained the VDR/DNA complex, free DNA, and free VDR. (D) Gel mobility shift of DNA in the presence of increasing concentrations of VDRm-NT (up to 8-fold molar excess) visualized by ethidium bromide staining. Lanes M in (B) and (D) contained 1 kb DNA ladder markers (Promega, Madison, WI), and lane M in (C): contained purified VDRm-NT.

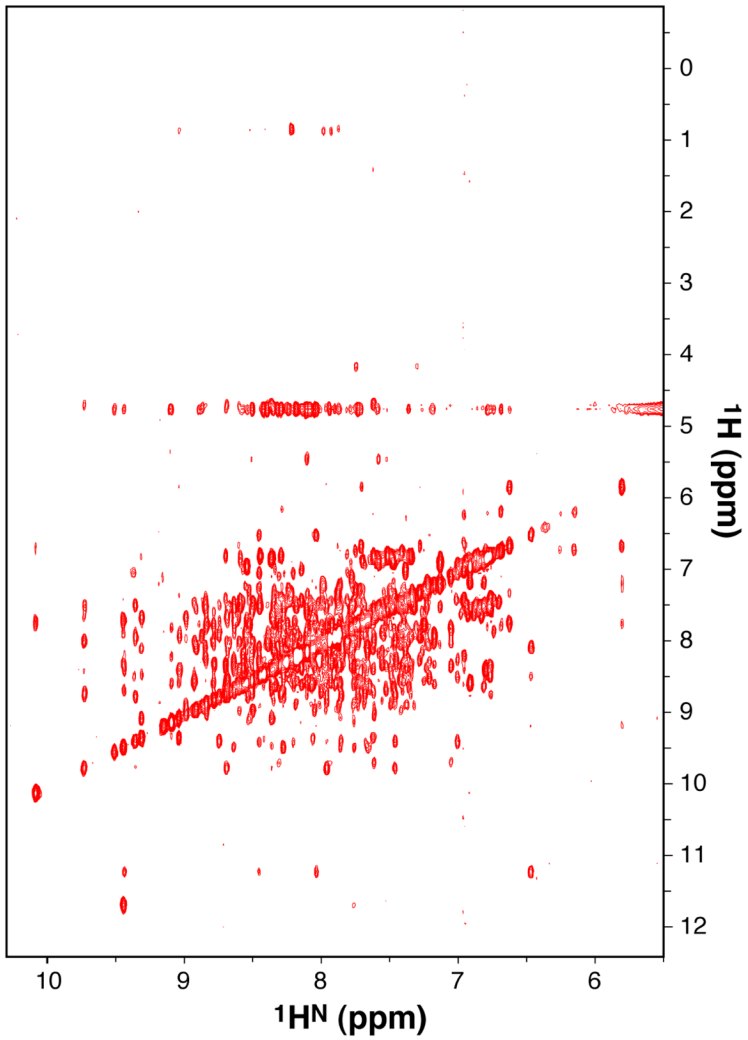

Figure 6.

Two-dimensional ^{1}H,^{1}H projection of a three-dimensional NOESY ^{1}H,^{15}N HSQC-TROSY spectrum of VDRm-NT. The regions containing NMR signals from aliphatic and amide/aromatic groups are shown. The contour levels are plotted down to the noise level. The lack of NOE cross-peaks between amide protons and aliphatic protons (~0–6ppm region) indicates that carbon-bound ^{1}H was replaced efficiently by ^{2}H. The remaining NOE cross-peaks are between amide protons. The number and spread of these cross-peaks in the amide region are indicative of a well folded protein. Note that the few peaks observed around 1 ppm are actually intermolecular NOEs between amide protons of VDR and a bound peptide, whereas the peaks at around 4.7 ppm are exchange peaks between amides and the bulk water solvent. The experiment was recorded on a 900 MHz Varian VNMRS spectrometer equipped with a cryogenic probe using a 0.5 mM protein sample in phosphate buffer, pH=7.4.

Table 1

Typical protein yield of VDRm-NT and LBDm-NT variants in LB

Protein expression:	**VDRm-NT (mg/L)**	**LBDm-NT (mg/L)**
Total lysate	506.5	408.2
Supernatant	358.6	266.8
Inclusion body pellet	147.9	141.4
Pellet after washing	134.0	132.1
Solubilized inclusion body	129.9	127.3
Final folded protein recovery after dialysis	32.2	35.3

Table 2

Ligand binding activity of VDR and LBD variants.

Receptor	K_d (× 10^{-10} M)
VDR	1.91 ± 0.17
VDRm	2.53 ± 0.48
VDRm-NT	2.32 ± 0.29
LBD	2.25 ± 0.33
LBDm	2.13 ± 0.25
LBDm-NT	1.96 ± 0.36